AGU ADVANCING EARTH AND SPACE SCIENCE

Geophysical Research Letters

RESEARCH LETTER
10.1029/2020GL091799

Key Points:

- Convective available potential energy (CAPE) can be predicted from environmental sounding parameters without lifting a hypothetical air parcel
- A step-by-step derivation demonstrates how CAPE scales with a recently proposed CAPE-like quantity
- A simple predictive linear equation is presented based on 20 years of reanalysis data over the U.S.

Supporting Information:

Supporting Information may be found in the online version of this article.

Correspondence to:
F. Li,
li3226@purdue.edu

Citation:
Li, F., & Chavas, D. R. (2021). Midlatitude continental CAPE is predictable from large-scale environmental parameters. *Geophysical Research Letters*, *48*, e2020GL091799. https://doi.org/10.1029/2020GL091799

Received 23 NOV 2020
Accepted 24 MAR 2021

Midlatitude Continental CAPE Is Predictable From Large-Scale Environmental Parameters

Funing Li[1] and Daniel R. Chavas[1]

[1]Department of Earth, Atmospheric, and Planetary Sciences, Purdue University, West Lafayette, IN, USA

Abstract A recent study by Agard and Emanuel (2017, https://doi.org/10.1175/jas-d-16-0352.1) proposed a simple equation for a quantity that scales with convective available potential energy (CAPE) that can be directly calculated from a limited number of environmental sounding parameters without lifting a hypothetical air parcel. This scaling CAPE was applied in a specific idealized framework, but the extent to which it can predict true CAPE in the real world has not been tested. This work uses reanalysis data over the U.S. to demonstrate that this scaling CAPE does indeed scale very closely with CAPE, following a linear relationship with a scaling factor of 0.44. We then explain why they scale together via a step-by-step derivation of the theoretical assumptions linking scaling CAPE and real CAPE and their manifestation in the historical data. Overall, this work demonstrates that CAPE can be predicted from large-scale environmental parameters alone, which may be useful for a wide range of applications in weather and climate.

Plain Language Summary Convective available potential energy (CAPE) is a key parameter commonly used to measure the potential for thunderstorms. Its calculation requires lifting a hypothetical air parcel through a column of atmosphere. This work combines theory and reanalysis data to demonstrate that CAPE can be predicted using environmental data alone. This can make it easier to quickly estimate CAPE in data and to understand the processes that create CAPE in our atmosphere.

1. Introduction

Convective available potential energy (CAPE), a measure of conditional instability of the environment, is a key thermodynamic parameter in atmospheric research. It is proportional to the theoretical maximum vertical wind speed within the atmospheric column and hence serves as an indicator of the potential intensity of deep convection if it is triggered (Holton, 1973). In practice, regular CAPE is estimated by the vertically integrated buoyancy of a boundary-layer parcel ascending from the level of free convection (LFC) to the equilibrium level (EL) (Doswell III & Rasmussen, 1994), given by

$$CAPE = \int_{zLFC}^{zEL} g\frac{T_{vp} - T_{ve}}{T_{ve}}dz \tag{1}$$

where g is the acceleration due to gravity, z is the height above ground level, T_{vp} is the virtual temperature of the rising air parcel and T_{ve} is that of the surrounding environment. Thus, calculating CAPE requires lifting a hypothetical parcel through a column of atmosphere defined by known vertical profiles of air temperature and moisture.

Recently, Agard and Emanuel (2017, hereafter AE17) proposed a simple equation for a quantity that scales with CAPE, here denoted $CAPE_{AE17}$, based on an idealized two-layer model for the atmospheric column. The AE17 model includes a dry adiabatic free troposphere overlying a cooler, moist, well-mixed boundary layer. Their proposed quantity scales with the difference between surface moist static energy (M_{ve}^{sfc}) and free tropospheric dry static energy ($\overline{D_{ve}^{FT}}$) multiplied by difference in the natural logarithm of virtual temperatures between boundary-layer top (T_{ve}^{BLT}) and tropopause (T_{ve}^{trop}):

$$CAPE_{AE17} = (M_{ve}^{sfc} - \overline{D_{ve}^{FT}})ln\frac{T_{ve}^{BLT}}{T_{ve}^{trop}} \tag{2}$$

The D_{ve} and M_{ve} are given by $D_{ve} = c_p T_{ve} + gz$ and $M_{ve} = c_p T_{ve} + gz + L_v r$, respectively, where c_p and L_v are the specific heat of the air and the latent heat of vaporization of water, and r is the water vapor mixing ratio. Note that Equation 2 is slightly different from the original formulation in AE17, as we use the free tropospheric mean dry static energy ($\overline{D_{ve}^{FT}}$) rather than a constant D_{ve} of the dry adiabatic free troposphere. In addition, we use virtual temperatures rather than temperatures for D_{ve} and M_{ve} to be consistent with definitions of CAPE in Equation 1 (detailed in Section 3). The CAPE_{AE17} formula suggests that CAPE may, to first order, be determined by a limited number of environmental parameters within the boundary layer and free troposphere. One significant benefit of this outcome is that this quantity may be calculated strictly from environmental sounding data without the need to lift a hypothetical air parcel.

Using this idealized framework, AE17 found that peak continental transient CAPE is expected to increase with global warming. Recent work used the AE17 framework to develop a simple physical model for a steady sounding for numerical simulations of severe convective storms (Chavas et al., 2020). However, it remains unclear to what extent CAPE_{AE17}, which represents CAPE in a highly idealized framework as we show below, directly predicts true CAPE in real soundings. Moreover, AE17 did not present a formal derivation of the relationship between CAPE_{AE17} and CAPE.

To fill this gap, this work seeks to answer the following question: How closely does CAPE_{AE17} scale with CAPE in real soundings, and why? To answer this question, we first directly compare CAPE_{AE17} with CAPE over the U.S. using reanalysis data and show that CAPE_{AE17} does indeed scale closely with regular CAPE (Section 2). We then provide a step-by-step theoretical derivation and application to sounding data to explain why they scale together (Section 3). We end with a summary and discussion (Section 4).

2. CAPE Versus CAPE_{AE17}

We begin with an explicit comparison of CAPE and CAPE_{AE17} in terms of (1) climatological extremes over the U.S., and (2) diurnal evolution during a significant tornado outbreak over the southern U.S.

2.1. Data

We use the 3-hourly surface and model-level (72 vertical levels) Modern-Era Retrospective analysis for Research and Applications version 2 (MERRA-2) reanalysis data for the period 2000–2019 in this work (Gelaro et al., 2017) (data accessed in March 2020 from https://disc.gsfc.nasa.gov/datasets/M2I1NXASM_5.12.4/summary for the surface data and from https://disc.gsfc.nasa.gov/datasets/M2I3NVASM_5.12.4/summary for the model-level data). The horizontal grid spacing of MERRA-2 is 0.5 ° × 0.65 ° in latitude and longitude. The model-level MERRA-2 data performs well in reproducing a reasonable magnitude and spatial distribution of CAPE over North America, though with a slight underestimation when compared against radiosonde data (Taszarek, Pilguj, et al., 2020). MERRA-2 also provides direct estimations of atmospheric properties at boundary-layer top and tropopause; this is especially useful for the calculation of CAPE_{AE17}. Tegtmeier et al. (2020) found realistic representations of MERRA-2 derived boundary-layer top and tropopause temperatures as compared to radiosonde observations, with a small mean bias of less than 1 K; this may induce a bias percentage of less than ~1% in CAPE_{AE17}. Our domain of analysis focuses on the contiguous U.S., as it is a major hot spot for severe thunderstorm environments in the world (Brooks et al., 2003).

We generate a 20-year dataset of CAPE using Equation 1 and CAPE_{AE17} using Equation 2 from the MERRA-2 reanalysis data over the U.S. Though CAPE estimation is sensitive to the origin of an air parcel, we select the near-surface parcel defined by 2-m temperature and moisture for simplicity, similar to past work (Li et al., 2020; Riemann-Campe et al., 2009; Seeley & Romps, 2015). Future work may seek to test alternate levels.

2.2. Results

We first compare the representation of the climatological spatial distribution of extreme values of CAPE_{AE17} against CAPE, as severe thunderstorms are typically associated with large values of CAPE (Brooks et al., 2003). We define extreme values by the 99th percentile of the full-period (2000–2019) time series of

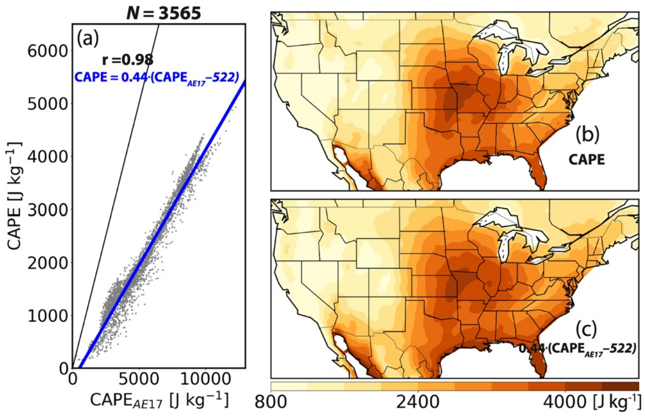

Figure 1. (a) Extreme values of CAPE (Equation 1) versus CAPE_{AE17} (Equation 2) over the contiguous U.S. Extreme values are defined as the 99th percentile of their respective full-period (2000–2019) time series from the MERRA-2 reanalysis data at each gridpoint (gray dots). The sample size is $N = 3{,}565$. Blue line denotes the linear least-squares fit with linear correlation coefficient (r). Black line denotes one-to-one fit. (b) Spatial distribution of extreme CAPE. (c) Predicted spatial distribution of extreme CAPE using the linear regression equation shown in (a).

a given quantity at each gridpoint, in line with past work (Li et al., 2020; Singh et al., 2017; Taszarek, Allen, et al., 2020; Tippett et al., 2016). Results show that extreme CAPE_{AE17} scales very closely with extreme CAPE (Figure 1a; $r = 0.98$), with linear regression given by

$$CAPE \approx 0.44\,(CAPE_{AE17} - 522) \tag{3}$$

We then apply Equation 3 to predicted extreme CAPE from extreme CAPE_{AE17} (Figure 1c), which produces a spatial pattern that is quantitatively very similar to the observed extreme CAPE (Figure 1b).

To further demonstrate how closely the two quantities scale, we present a case study comparison of their diurnal evolution during April 25, 2011, which is the first day of a three-day significant tornado outbreak event in the southeastern U.S. (Knupp et al., 2014). The diurnal variation of CAPE indicates an initial generation of CAPE over southeastern Texas in the early morning (0900–1200 UTC; Figures 2a and 2b), followed by a strong enhancement at around 1500 UTC over eastern Texas (Figure 2c) and an eastward propagation of high CAPE in the afternoon (Figures 2d–2f). The high CAPE values in the afternoon–evening over the southeastern U.S. are associated with a swath of over 50 tornado reports extending from eastern Texas into the mid-Mississippi Valley (reference to the SPC Storm Reports: https://www.spc.noaa.gov/exper/archive/event.php?date=20110425). Compared to CAPE, CAPE_{AE17} successfully reproduces the detailed spatial patterns and diurnal variations during the day (Figures 2g–2l), with pattern correlation $r \geq 0.90$ at each UTC time, though Equation 3 slightly overestimates CAPE in the morning (Figures 2g and 2h vs. Figures 2a and 2b) and slightly underestimates CAPE in the afternoon (Figures 2j and 2k vs. Figures 2d and 2e).

Overall, our comparisons for both climatological extremes and the diurnal variation associated with a tornado outbreak case demonstrate a tight relationship between CAPE_{AE17} and CAPE distributions. This indicates that CAPE can be approximately predicted from CAPE_{AE17} via a simple linear equation. While this section focused on extreme values of CAPE to demonstrate its spatial variability, we show in Section 3 that such a close linear relation between CAPE and CAPE_{AE17} extends to the full distribution of CAPE.

3. Theoretical Foundation

We next provide a theoretical derivation and explanation of the intermediate steps and assumptions that link CAPE to CAPE_{AE17}. We demonstrate each step both for a single example radiosonde sounding (Figure 3) and statistically for all U.S. gridpoints in the full-period (2000–2019) MERRA-2 reanalysis database (Figure 4). Here, the example sounding was observed at 0000 UTC June 07, 2011 at the SGF (Springfield, MO) station; we obtain it from the sounding database of the University of Wyoming (http://weather.uwyo.edu/upperair/sounding.html).

3.1. A Dry Static Energy View of CAPE

As CAPE_{AE17} is a function of an environmental static energy surplus between the boundary layer and free troposphere, we first derive an alternative formula for estimating CAPE based on the parcel and environmental profiles of dry static energy rather than temperature.

We begin from the environmental dry static energy relation (D_{ve}), $D_{ve} = c_p T_{ve} + gz$. The environmental moist static energy (M_{ve}) is given by $M_{ve} = c_p T_{ve} + gz + L_v r$. Heat capacities and latent heats are assumed to be constant. Counterparts for the parcel are given by D_{vp} and M_{vp}. Note that these static energies include the virtual temperature effect to be consistent with definitions of CAPE in Equation 1. This virtual effect may add a small positive perturbation to regular static energies of approximately 0.9% and 0.8% of near-surface dry and moist static energy, respectively, given a surface temperature of 300 K and mixing ratio of 15 g kg^{-1}, that will decrease with height. We rewrite the D_{ve} equation for differential changes in height z as

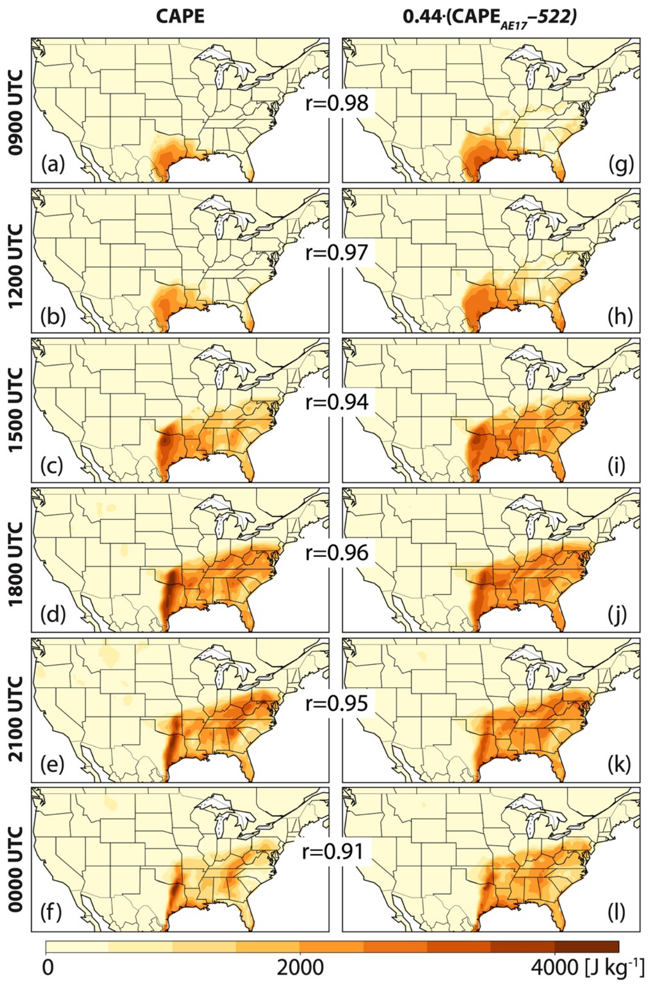

Figure 2. Spatial distributions of (a–f) CAPE versus (g–l) predicted CAPE, using the equation in Figure 1a, at (top–bottom) 0900, 1200, 1500, 1800, 2100, and 0000 UTC on April 25, 2011 from the MERRA-2 reanalysis data. The r denotes the pattern correlation coefficient between CAPE and $CAPE_{AE17}$ conditioned on gridpoints with CAPE ≥ 100 J kg^{-1}.

$dz = -\frac{c_p}{g}dT_{ve} + \frac{1}{g}dD_{ve}$ and substitute into Equation 1. Doing so yields an alternative formulation of CAPE with limited approximations based on dry static energy profiles of the rising air parcel and the environment (derivation in Appendix A):

$$CAPE \approx \frac{\Gamma_d}{\Gamma}\mathcal{D} = -\frac{\Gamma_d}{\Gamma}\int_{T_{ve}^{LFC}}^{T_{ve}^{EL}}(D_{vp} - D_{ve})dlnT_{ve} \tag{4}$$

where $\Gamma_d = g/c_p$ is the dry adiabatic lapse rate, Γ is the virtual temperature lapse rate of the environment from LFC to EL, and T_{ve}^{LFC} and T_{ve}^{EL} are environmental virtual temperatures at LFC and EL, respectively.

How well does $\frac{\Gamma_d}{\Gamma}\mathcal{D}$ (Equation 4) compare to CAPE (Equation 1)? First, we compare $\frac{\Gamma_d}{\Gamma}\mathcal{D}$ against CAPE for our example sounding (Figure 3 inset). The two calculations yield similar values of CAPE (3,775 vs. 3,902 J kg^{-1}). The slightly high bias in $\frac{\Gamma_d}{\Gamma}\mathcal{D}$ relative to CAPE (+3.4%) is due to the assumption of constant environmental virtual temperature lapse rate (Γ) from LFC to EL (Equation A5). Second, we compare the two quantities for all gridpoints over the U.S in our MERRA-2 reanalysis dataset. The two quantities are indeed nearly identical (Figure 4a; $r > 0.99$) with linear regression given by CAPE= $0.98(\frac{\Gamma_d}{\Gamma}\mathcal{D} + 18)$. The $\frac{\Gamma_d}{\Gamma}\mathcal{D}$ formulation performs equally well in reproducing the detailed spatial distribution of extreme CAPE over the U.S. (Figure S1b vs. Figure S1a).

3.2. Scaling of CAPE with $CAPE_{AE17}$

To obtain the $CAPE_{AE17}$ formula from Equation 4, we must assume that $D_{vp} = M_{ve}^{sfc}$, which yields

$$\frac{\Gamma_d}{\Gamma}\mathcal{D}_{AE17} = \frac{\Gamma_d}{\Gamma}(M_{ve}^{sfc} - \overline{D_{ve}})ln\frac{T_{ve}^{LFC}}{T_{ve}^{EL}} \tag{5}$$

where $\overline{D_{ve}} = \frac{\int_{T_{ve}^{LFC}}^{T_{ve}^{EL}}\left(D_{ve}\right)dlnT_{ve}}{\int_{T_{ve}^{LFC}}^{T_{ve}^{EL}}dlnT_{ve}}$ is the log-temperature-weighted average dry static energy of environment between LFC and EL. Though this assumption is not made explicitly in AE17, it is an essential inference in order to derive $CAPE_{AE17}$ for a real atmosphere. Physically, this assumption implies that the lifted air parcel immediately converts all latent heat to sensible heat at LFC. Hence, the parcel will experience a sudden jump in dry static energy D_{vp} (to be equal to M_{vp}) at the LFC, and above the LFC this quantity is conserved. Additionally, we must assume that the moist static energy of the surface parcel is conserved up to the LFC. Note that static energy is not perfectly conserved during adiabatic ascent because buoyancy acts as an enthalpy sink (Romps, 2015); because this static energy sink is not accounted for, the idealized parcel (Figure 3 black dashed) ends at a higher adiabat than the parcel following the regular moist adiabat (Figure 3 black solid). Taken together, the assumption results in $D_{vp} = M_{vp} = M_{ve}^{sfc}$.

We further use our example sounding (Figure 3) to help understand this assumption conceptually. As noted above, the above assumption implies that all latent heat within an air parcel is immediately converted to sensible heat at the LFC. Thus, the parcel is immediately warmed dramatically at the LFC and then

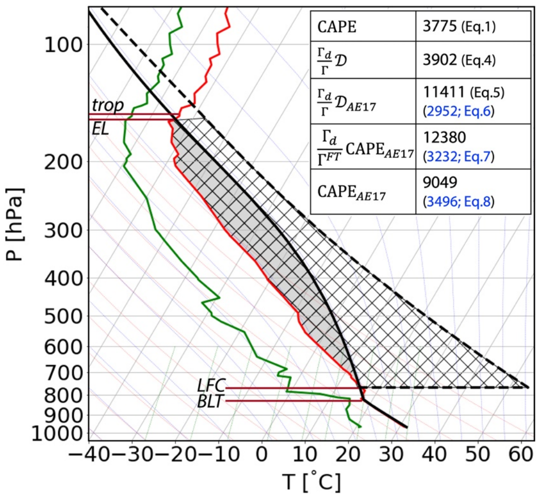

Figure 3. The SGF (Springfield, MO) radiosonde observed virtual temperature (in red line) and dew-point temperature (in green line) profiles at 0000 UTC June 07, 2011 in a Skew-T diagram. Solid black line represents the virtual temperature profile of a surface air parcel ascending adiabatically. Dashed black line represents the virtual temperature profile of the idealized parcel ascending assuming that it converts all latent heat immediately to virtual dry static energy at LFC and perfectly conserves its virtual dry static energy thereafter. The *EL*, *LFC*, *trop*, and *BLT* are denoted by brown lines. Inset table lists values of CAPE (grey shading; Equation 1); $\frac{\Gamma_d}{\Gamma}\mathcal{D}$ (Equation 4); $\frac{\Gamma_d}{\Gamma}\mathcal{D}_{AE17}$ (Equation 5; approximates hatched region area = 10,944 J kg^{-1}); $\frac{\Gamma_d}{\Gamma^{FT}}\mathrm{CAPE}_{AE17}$ is the same as $\frac{\Gamma_d}{\Gamma}\mathcal{D}_{AE17}$ but using virtual temperatures at *BLT* and *trop*, with CAPE_{AE17} calculated from Equation 2. The inset table lists the direct calculation of each quantity (black text) and prediction of true CAPE (blue text) using the relevant linear regression equation. The Python MetPy (May et al., 2008–2020) package is used to generate the parcel temperature profiles.

subsequently rises dry adiabatically from the LFC to the EL. In this way, then, $\frac{\Gamma_d}{\Gamma}\mathcal{D}_{AE17}$ is considered a "scaling" CAPE because it represents a theoretical upper bound on how quickly a parcel can be warmed along its path (and hence on its integrated buoyancy). In the real atmosphere, latent heat is released gradually along the parcel path in accordance with the Clausius–Clapeyron relation that defines the moist adiabatic lapse rate. In a Skew-T diagram (Figure 3), this difference shows up as an expanded, angular region of positive buoyancy maximized above the LFC in $\frac{\Gamma_d}{\Gamma}\mathcal{D}_{AE17}$, which is larger than the true CAPE area. Thus, $\frac{\Gamma_d}{\Gamma}\mathcal{D}_{AE17}$ is substantially larger than CAPE: $\frac{\Gamma_d}{\Gamma}\mathcal{D}_{AE17}$ =11,411 J kg^{-1} versus CAPE = 3,775 J kg^{-1} (Figure 3 inset). $\frac{\Gamma_d}{\Gamma}\mathcal{D}_{AE17}$ is slightly larger (+4.2%) than the true value given by the hatched area (10,944 J kg^{-1}), due to the assumption of constant Γ as noted earlier.

Though different in magnitude, $\frac{\Gamma_d}{\Gamma}\mathcal{D}_{AE17}$ is still highly correlated with CAPE (r = 0.92) in the full reanalysis dataset over the U.S. (Figure 4b), with linear regression given by

$$CAPE \approx 0.32\left(\frac{\Gamma_d}{\Gamma}\mathcal{D}_{AE17} - 2188\right) \tag{6}$$

For the example sounding, Equation 6 predicts a CAPE value (2,952 J kg^{-1}) that is reasonably close to the true CAPE (3,775 J kg^{-1}) (Figure 3, inset). Equation 6 also performs very well in reproducing the spatial distribution of extreme CAPE over the U.S. (Figure S1c vs. Figure S1a). Physically, the factor 0.32 is a manifestation of the large difference in the temperature profile of the parcel as it rises for the idealized parcel as compared to the normal parcel profile following the standard moist adiabatic lapse rate. The latter is a manifestation of the Clausius–Clapeyron relation governing the rate at which condensation occurs as the parcel cools adiabatically, and hence the rate at which latent heat is gradually converted to sensible heat (dry static energy) as the parcel rises through the troposphere. This contrasts with the idealized parcel where D_{vp} is set equal to M_{vp} immediately at the LFC, which equates to an instantaneous conversion of all latent heat to dry static energy. Geometrically, the factor 0.32 visually represents the ratio of the true CAPE area (grey shading in Figure 3) to the idealized parcel CAPE area (hatched in Figure 3). Indeed, for the case shown in Figure 3, that ratio is 0.33.

Finally, to produce a prediction with the original AE17 formulation (CAPE_{AE17}), we must additionally assume that the temperatures of the EL and LFC may be replaced with that of the tropopause (*trop*) and boundary-layer top (*BLT*), respectively. This replaces $\frac{\Gamma_d}{\Gamma}\mathcal{D}_{AE17}$ of Equation 5 with $\frac{\Gamma_d}{\Gamma^{FT}}\mathrm{CAPE}_{AE17}$, where Γ^{FT} is defined by the lapse rate of virtual temperature of the free troposphere between the *BLT* and *trop*. These approximations are more quantitatively reasonable for higher-CAPE cases supportive of deep convection, as in the example sounding (Figure 3). This final approximation ($\frac{\Gamma_d}{\Gamma^{FT}}\mathrm{CAPE}_{AE17}$) is estimated solely by environmental parameters without lifting a hypothetical air parcel. We use the reanalysis dataset to examine its relationship to CAPE (Figure 4c), which indicates a close correlation (r = 0.86) with a linear regression given by

$$CAPE \approx 0.30\left(\frac{\Gamma_d}{\Gamma^{FT}}CAPE_{AE17} - 1608\right) \tag{7}$$

10.1029/2020GL091799

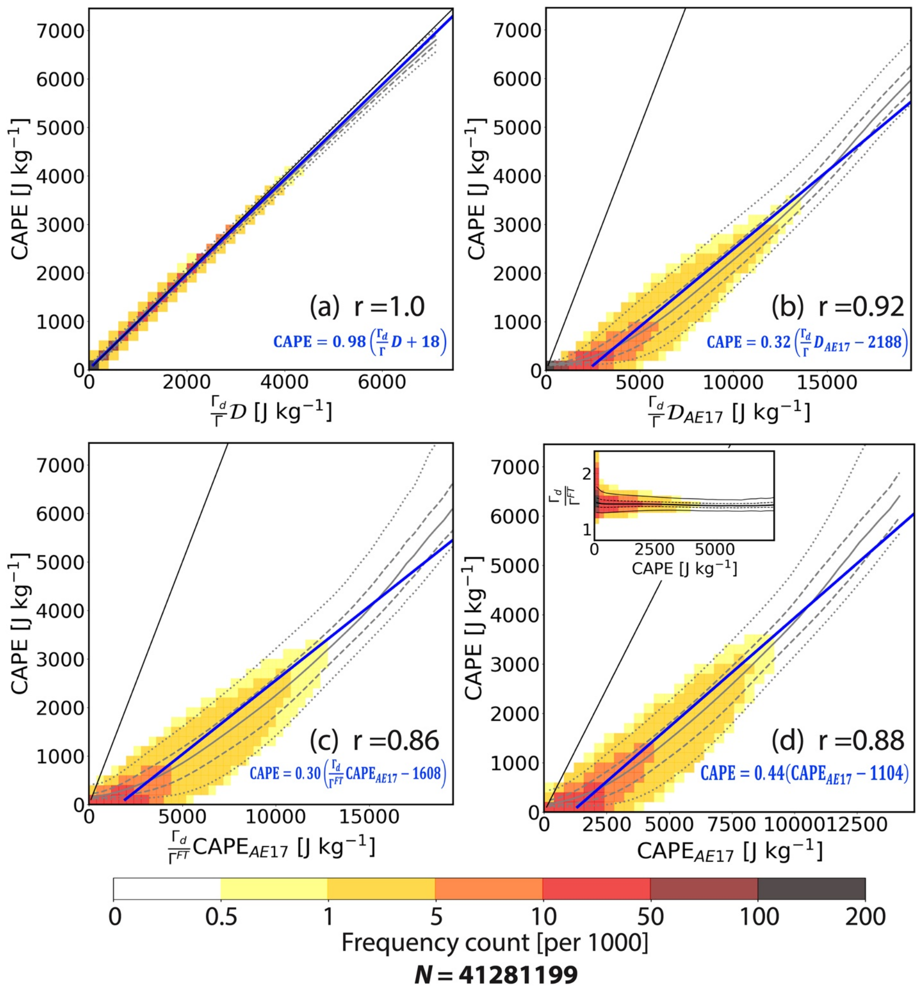

Figure 4. Joint frequency fraction multiplied by 1,000 (filled color) of (a) CAPE versus $\frac{\Gamma_d}{\Gamma}\mathcal{D}$, (b) CAPE versus $\frac{\Gamma_d}{\Gamma}\mathcal{D}_{AE17}$, (c) CAPE versus $\frac{\Gamma_d}{\Gamma^{FT}}\text{CAPE}_{AE17}$, and (d) CAPE versus CAPE_{AE17} (inset: $\frac{\Gamma_d}{\Gamma^{FT}}$ vs. CAPE) for cases with CAPE ≥ 100 J kg^{-1} over all U.S. gridpoints during 2000–2019 from the MERRA-2 reanalysis dataset (sample size N = 41,281,199). Black line denotes one-to-one line. Gray lines denote median (solid), interquartile range (dashed), and 5%–95% range (dotted) of CAPE. Blue line denotes the linear regression with the correlation coefficient of r.

Hence, the scaling factor is similar to that for $\frac{\Gamma_d}{\Gamma}\mathcal{D}_{AE17}$ above. For our example sounding, Equation 7 predicts a CAPE value (3,232 J kg^{-1}) again reasonably close to the true CAPE (3,775 J kg^{-1}) (Figure 3 insert). Equation 7 also quantitatively reproduces the spatial pattern of extreme CAPE over the U.S. (Figure S1d vs. Figure S1a).

Ultimately, then, Equation 7 offers a scaling of CAPE that depends only on a limited number of boundary-layer and free tropospheric variables. It differs from CAPE_{AE17} itself in the inclusion of the coefficient $\frac{\Gamma_d}{\Gamma^{FT}}$. This factor does not appear in the idealized model of AE17 because their model assumes a dry adiabatic free troposphere (i.e., $\Gamma^{FT} = \Gamma_d$), which yields $\frac{\Gamma_d}{\Gamma^{FT}} = 1$.

Given that CAPE was found to be predictable from CAPE_{AE17} alone in Section 2 (Equation 3), this result implies that the free tropospheric lapse rate (Γ^{FT}) of the modern atmosphere does not vary too strongly and thus the factor $\frac{\Gamma_d}{\Gamma^{FT}}$ remains relatively constant. We use our reanalysis dataset to calculate the statistics of

$\frac{\Gamma_d}{\Gamma^{FT}}$ as a function of CAPE (Figure 4d inset). The result is indeed a mean (±one standard deviation) value of 1.47 ± 0.06, with variance decreasing as CAPE increases. The resulting mean free tropospheric lapse rate (Γ^{FT}) is roughly 6.7 K km^{-1}, which is close to that of the U.S. Standard Atmosphere (COESA, 1976). These results indicate a relatively constant free tropospheric thermal structure at high values of CAPE, a result that is worthy of deeper investigation. As a result, we are able to directly scale CAPE with CAPE$_{AE17}$ by assuming that $\frac{\Gamma_d}{\Gamma^{FT}}$ is constant. We note that this behavior may differ in an alternate climate state. As a final test, we compare CAPE$_{AE17}$ with CAPE for cases with CAPE ≥ 100 J kg^{-1} for the entire MERRA-2 database over the U.S. and find a strong linear correlation between them as well (r = 0.88; Figure 4d), with a linear regression of

$$CAPE \approx 0.44(CAPE_{AE17} - 1104). \tag{8}$$

This outcome is quite similar to the linear regression model we get from extreme cases alone in Equation 3. This is also close to the results of simply substituting $\frac{\Gamma_d}{\Gamma^{FT}} = 1.47 \pm 0.06$ into Equation 7, which yields a scaling factor of 0.44 ± 0.02 and an offset of −1095 ± 50. Using Equation 8 also successfully predicts the approximate CAPE for the example sounding (3,496 vs. 3,775 J kg^{-1}; Figure 3 inset).

4. Conclusions

CAPE is a key thermodynamic parameter commonly calculated to evaluate the potential for deep convection within a given environment. AE17 proposed a simple formula for a quantity (CAPE$_{AE17}$) that scales with CAPE that depends only on a limited number of environmental variables and does not require lifting a hypothetical parcel. CAPE$_{AE17}$ represents an expression of CAPE for a highly idealized column in which the EL and LFC are exactly the tropopause and boundary-layer tops, the free tropospheric lapse rate is dry adiabatic, and the rising parcel instantly converts all latent heat to sensible heat at LFC; this requires idealizations of both the environmental and parcel thermal profiles.

This work used a 20-year reanalysis dataset over the U.S. to examine the extent to which this CAPE-like quantity can be used to predict true CAPE for real soundings, analyzing both the spatial distribution of climatological extremes and the diurnal variation associated with a historical tornado outbreak case study. Results show a close scaling relationship between CAPE$_{AE17}$ and CAPE, yielding a simple linear equation for predicting CAPE from environmental data. To understand the physics underlying this relationship, we provided a step-by-step derivation linking the two quantities, which may be summarized as:

$$CAPE \overset{a1}{\approx} \frac{\Gamma_d}{\Gamma}\mathcal{D} \overset{a2}{\sim} \frac{\Gamma_d}{\Gamma}\mathcal{D}_{AE17} \overset{a3}{\sim} \frac{\Gamma_d}{\Gamma^{FT}} CAPE_{AE17} \overset{a4}{\sim} CAPE_{AE17} \tag{9}$$

where (a1–a4) represent the assumptions: (a1) constant environmental virtual temperature lapse rate from LFC to EL; (a2) the rising parcel immediately converts all latent heat to sensible heat at the LFC; (a3) temperatures at the EL and LFC are equal to the tropopause and boundary-layer top, respectively; (a4) free tropospheric lapse rate of the present atmosphere does not vary strongly in space or time in environments with non-negligible CAPE.

Though our assessment focused on the U.S. continent, CAPE$_{AE17}$ also performs well in predicting CAPE over the Gulf of Mexico and nearby tropical ocean (Figures S2a–S2l). Additionally, we examined an existing analytical prediction for mean CAPE in the tropics (CAPE$_{R16}$; Equation 17 in Romps [2016]), which also depends only on environmental parameters. We find that CAPE$_{R16}$ does not reproduce the detailed spatial distribution and temporal evolution of high CAPE values for the case study over the U.S. continent, though the performance is slightly improved over the ocean (Figures S2m–S2r). The derivation of CAPE$_{R16}$ assumes a zero-buoyancy plume under radiative–convective equilibrium. This assumption applies very well for describing the tropical mean state, which is governed principally by the upward transfer of heat and moisture by persistent deep convection (and its associated entrainment) that allows for an accurate prediction of the free tropospheric thermodynamic structure from surface air properties alone. However, continental convective environments involve the time-dependent buildup and storage of CAPE due to the presence of significant convective inhibition generated by the superposition of distinct air masses as well as variability in land surface-air interactions (Agard & Emanuel, 2017; Carlson et al., 1983; Romps, 2014, 2016; Singh & O'Gorman, 2013). Hence, CAPE_{R16} would not be expected to perform well in such environments.

This work has significant practical benefits for the simple estimation of CAPE and for understanding the processes that create CAPE in our atmosphere. The principal end result of this work is a simple linear equation based on the 20-year reanalysis dataset over the U.S. (Equation 8) to predict CAPE from CAPE_{AE17}, which may be calculated strictly from environmental data without the need to lift a hypothetical parcel. Meanwhile, the close relationship between CAPE and CAPE_{AE17} indicates that there is significant potential to use CAPE_{AE17} to understand how CAPE is generated within the climate system. This includes quantifying the roles of variability in surface moist static energy, free tropospheric dry static energy, and temperatures at the top of the boundary layer and tropopause and the processes that govern each. This is a promising avenue of future research.

Appendix A: Derivation of Equation 4

The equation for differential changes in environmental dry static energy is written as $dz = -\frac{c_p}{g}dT_{ve} + \frac{1}{g}dD_{ve}$ and substituting into Equation 1 yields

$$CAPE = \int_{zLFC}^{zEL} g\frac{T_{vp} - T_{ve}}{T_{ve}}\left(-\frac{c_p}{g}dT_{ve} + \frac{1}{g}dD_{ve}\right) = \mathcal{D} + \mathcal{T} \tag{A1}$$

This formulation decomposes CAPE into two terms. The first is given by

$$\mathcal{D} = -\int_{zLFC}^{zEL}\left(\frac{T_{vp} - T_{ve}}{T_{ve}}\right)d(c_pT_{ve}) = -\int_{zLFC}^{zEL}(D_{vp} - D_{ve})dlnT_{ve} \tag{A2}$$

and represents differences in dry static energy integrated over changes in temperature. The second is given by

$$\mathcal{T} = \int_{zLFC}^{zEL}\left(\frac{T_{vp} - T_{ve}}{T_{ve}}\right)dD_{ve} \tag{A3}$$

and represents integrated differences in temperature over changes in dry static energy. To further simplify Equation A1, we can relate $\mathcal{T}$ and $\mathcal{D}$ by calculating their ratio. Using the definition of buoyancy, $b = \frac{T_{vp} - T_{ve}}{T_{ve}}$, we may write this ratio as

$$\begin{aligned}\frac{\mathcal{T}}{\mathcal{D}} &= \frac{\int_{zLFC}^{zEL}(b)\,dD_{ve}}{-\int_{zLFC}^{zEL}(b)\,d(c_pT_{ve})}\\ &= -\left(1 + \frac{g}{c_p}\frac{\int_{zLFC}^{zEL}(b)\,dz}{\int_{zLFC}^{zEL}(b)\,dT_{ve}}\right)\\ &= -\left(1 + \frac{g}{c_p}\frac{\overline{b_1}\int_{zLFC}^{zEL}dz}{\overline{b_2}\int_{zLFC}^{zEL}dT_{ve}}\right)\\ &= \frac{\overline{b_1}}{\overline{b_2}}\frac{\Gamma_d}{\Gamma} - 1\end{aligned} \tag{A4}$$

where $\overline{b_1} = \frac{\int_{zLFC}^{zEL}(b)\,dz}{\int_{zLFC}^{zEL}dz}$ and $\overline{b_2} = \frac{\int_{zLFC}^{zEL}(b)\,dT_{ve}}{\int_{zLFC}^{zEL}dT_{ve}}$ represent the mean value of b between the LFC and EL weighted by height (z) and environmental virtual temperature (T_{ve}), respectively. $\Gamma_d = g/c_p$ is the dry adiabatic lapse rate and $\Gamma = -\frac{\int_{zLFC}^{zEL}dT_{ve}}{\int_{zLFC}^{zEL}dz} = -\frac{T_{ve}^{EL} - T_{ve}^{LFC}}{z_{EL} - z_{LFC}}$ represents the average environmental virtual temperature lapse rate from LFC to EL.

If we take Γ to be constant between the LFC and EL, then $\overline{b_1} = \overline{b_2}$, which yields

$$\frac{\mathcal{T}}{\mathcal{D}} = \frac{\Gamma_d}{\Gamma} - 1 \tag{A5}$$

Substituting this result into Equation A1 yields

$$CAPE \approx \frac{\Gamma_d}{\Gamma}\mathcal{D} = -\frac{\Gamma_d}{\Gamma}\int_{zLFC}^{zEL}(D_{vp} - D_{ve})dlnT_{ve} \tag{A6}$$

This equation is shown to closely match the true CAPE in the main manuscript.

Data Availability Statement

The surface and model-level MERRA-2 reanalysis data during 2000–2019 were downloaded from https://disc.gsfc.nasa.gov/datasets/M2I1NXASM_5.12.4/summary (http://doi.org/10.5067/3Z173KIE2TPD) and https://disc.gsfc.nasa.gov/datasets/M2I3NVASM_5.12.4/summary (http://doi.org/10.5067/WWQSXQ8IVFW8), respectively. The example sounding was obtained from the sounding database of the University of Wyoming at http://weather.uwyo.edu/upperair/sounding.html.

Acknowledgments

The authors thank Vince Agard, an anonymous reviewer, and the editor for insightful and constructive feedback. The authors acknowledge high-performance computing support from Cheyenne (https://doi.org/10.5065/D6RX99HX) provided by NCAR's Computational and Information Systems Laboratory, sponsored by the National Science Foundation, for the data analysis performed in this work. The authors gratefully acknowledge the open-source Python community, and particularly the authors and contributors to the Matplotlib (Hunter, 2007), NumPy (Oliphant, 2006), and MetPy (May et al., 2008–2020) packages that were used to generate many of the figures. F. Li and D. R. Chavas were supported by NASA FINESST Grant 12000365 and NSF Grant 1648681.

References

Agard, V., & Emanuel, K. (2017). Clausius–Clapeyron Scaling of Peak CAPE in Continental Convective Storm Environments. *Journal of the Atmospheric Sciences*, *74*(9), 3043–3054. https://doi.org/10.1175/jas-d-16-0352.1

Brooks, H. E., Lee, J. W., & Craven, J. P. (2003). The spatial distribution of severe thunderstorm and tornado environments from global reanalysis data. *Atmospheric Research*, *67*, 79–94. https://doi.org/10.1016/S0169-8095(03)00045-0

Carlson, T. N., Benjamin, S. G., Forbes, G. S., & Li, Y.-F. (1983). Elevated mixed layers in the regional severe storm environment: Conceptual model and case studies. *Monthly Weather Review*, *111*(7), 1453–1474. https://doi.org/10.1175/1520-0493(1983)111<1453:emlitr>2.0.co;2

Chavas, D. R., Dawson, I., & Daniel, T. (2020). An idealized physical model for the severe convective storm environmental sounding. *Journal of the Atmospheric Sciences*, *78*(2), 653–670. https://doi.org/10.1175/JAS-D-20-0120.1

COESA. (1976). U.S. standard atmosphere. *National Oceanic and Atmospheric Administration*, *76*(1562), 227.

Doswell, C. A., III, & Rasmussen, E. N. (1994). The effect of neglecting the virtual temperature correction on CAPE calculations. *Weather Forecasting*, *9*(4), 625–629. https://doi.org/10.1175/1520-0434(1994)009<0625:teontv>2.0.co;2

Gelaro, R., McCarty, W., Suárez, M. J., Todling, R., Molod, A., Takacs, L., et al. (2017). The modern-era retrospective analysis for research and applications, version 2 (MERRA-2). *Journal of Climate*, *30*(14), 5419–5454. https://doi.org/10.1175/jcli-d-16-0758.1

Holton, J. R., & Staley, D. O. (1973). An introduction to dynamic meteorology. *American Journal of Physics*, *41*(5), 752–754. https://doi.org/10.1119/1.1987371

Hunter, J. D. (2007). Matplotlib: A 2d graphics environment. *Computing in Science and Engineering*, *9*(3), 90–95. https://doi.org/10.1109/MCSE.2007.55

Knupp, K. R., Murphy, T. A., Coleman, T. A., Wade, R. A., Mullins, S. A., Schultz, C. J., et al. (2014). Meteorological overview of the devastating 27 April 2011 tornado outbreak. *Bulletin of the American Meteorological Society*, *95*(7), 1041–1062. https://doi.org/10.1175/bams-d-11-00229.1

Li, F., Chavas, D. R., Reed, K. A., & Dawson, D. T., II (2020). Climatology of severe local storm environments and synoptic-scale features over North America in ERA5 reanalysis and CAM6 simulation. *Journal of Climate*. https://doi.org/10.1175/JCLI-D-19-0986.1

May, R. M., Arms, S. C., Marsh, P., Bruning, E., Leeman, J. R., Goebbert, K., et al. (2008–2020). *Metpy: A Python package for meteorological data*. Unidata. https://doi.org/10.5065/D6WW7G29

Oliphant, T. E. (2006). A Guide to NumPy (Vol. 1), Trelgol Publishing.

Riemann-Campe, K., Fraedrich, K., & Lunkeit, F. (2009). Global climatology of convective available potential energy (CAPE) and convective inhibition (CIN) in ERA-40 reanalysis. *Atmospheric Research*, *93*(1–3), 534–545. https://doi.org/10.1016/j.atmosres.2008.09.037

Romps, D. M. (2014). An analytical model for tropical relative humidity. *Journal of Climate*, *27*(19), 7432–7449. https://doi.org/10.1175/jcli-d-14-00255.1

Romps, D. M. (2015). MSE minus CAPE is the true conserved variable for an adiabatically lifted parcel. *Journal of the Atmospheric Sciences*, *72*(9), 3639–3646. https://doi.org/10.1175/jas-d-15-0054.1

Romps, D. M. (2016). Clausius-Clapeyron scaling of CAPE from analytical solutions to RCE. *Journal of the Atmospheric Sciences*, *73*(9), 3719–3737. https://doi.org/10.1175/jas-d-15-0327.1

Seeley, J. T., & Romps, D. M. (2015). The effect of global warming on severe thunderstorms in the United States. *Journal of Climate*, *28*(6), 2443–2458. https://doi.org/10.1175/jcli-d-14-00382.1

Singh, M. S., Kuang, Z., Maloney, E. D., Hannah, W. M., & Wolding, B. O. (2017). Increasing potential for intense tropical and subtropical thunderstorms under global warming. *Proceedings of the National Academy of Sciences of the United States of America*, *114*(44), 11657–11662. https://doi.org/10.1073/pnas.1707603114

Singh, M. S., & O'Gorman, P. A. (2013). Influence of entrainment on the thermal stratification in simulations of radiative-convective equilibrium. *Geophysical Research Letters*, *40*(16), 4398–4403. https://doi.org/10.1002/grl.50796

Taszarek, M., Allen, J. T., Púčik, T., Hoogewind, K. A., & Brooks, H. E. (2020). Severe convective storms across Europe and the United States. Part 2: ERA5 environments associated with lightning, large hail, severe wind and tornadoes. *Journal of Climate*, 1–53. https://doi.org/10.1175/JCLI-D-20-0346.1

Taszarek, M., Pilguj, N., Allen, J. T., Gensini, V., Brooks, H. E., & Szuster, P. (2020). Comparison of convective parameters derived from era5 and merra2 with Rawinsonde data over Europe and North America. *Journal of Climate*, 1–55. https://doi.org/10.1175/jcli-d-20-0484.1

Tegtmeier, S., Anstey, J., Davis, S., Dragani, R., Harada, Y., Ivanciu, I., et al. (2020). Temperature and tropopause characteristics from reanalyses data in the tropical tropopause layer. *Atmospheric Chemistry and Physics*, *20*(2), 753–770. https://doi.org/10.5194/acp-20-753-2020

Tippett, M. K., Lepore, C., & Cohen, J. E. (2016). More tornadoes in the most extreme U.S. tornado outbreaks. *Science*, *354*(6318), 1419–1423. https://doi.org/10.1126/science.aah7393